HINDERED DIFFUSION OF CONFINED HARD-SPHERE FLUIDS IN CYLINDRICAL PORES

SOONG-HYUCK SUH AND SEUNG-BAIK RHO
Department of Chemical Engineering, Keimyung University, Taegu 704-701, Korea
SOON-CHUL KIM
Department of Physics, Andong National University, Andong 760-749, Korea

Key Words: Molecular Dynamics Simulation, Hard-Sphere Fluid, Cylindrical Pore, Hindered Diffusion Coefficient, Collision Frequency

Introduction

During the last two decades, molecular-based computer simulations have provided the most satisfactory basis for our understanding and interpretation of inhomogeneous fluids in restricted pore geometries. The most widely employed model systems in these simulation studies[1] have been slit, cylindrical, and spherical pores. The only input information required in performing machine experiments (computer simulations), apart from some fixed initial parameters, is the description of interacting potentials for precisely defined systems.

Received January 27. 1993. Correspondence concerning this article should be addressed to S. -H. Suh.

In many cases the molecular size exclusion of confined fluids significantly influences hindered-diffusion fluxes, particularly when the size of diffusing molecules is commensurate with that of porous media[2]. One of the major consequences recently observed in liquid-filled micropores[3] is a severe reduction in solute diffusional transport rates. For a simple pore model of nonadsorbing solutes, continuum-mechanical approaches based on hydrodynamic concepts allow the theoretical prediction of equilibrium and transport properties[4,5].

In this study we investigate the hindered diffusion

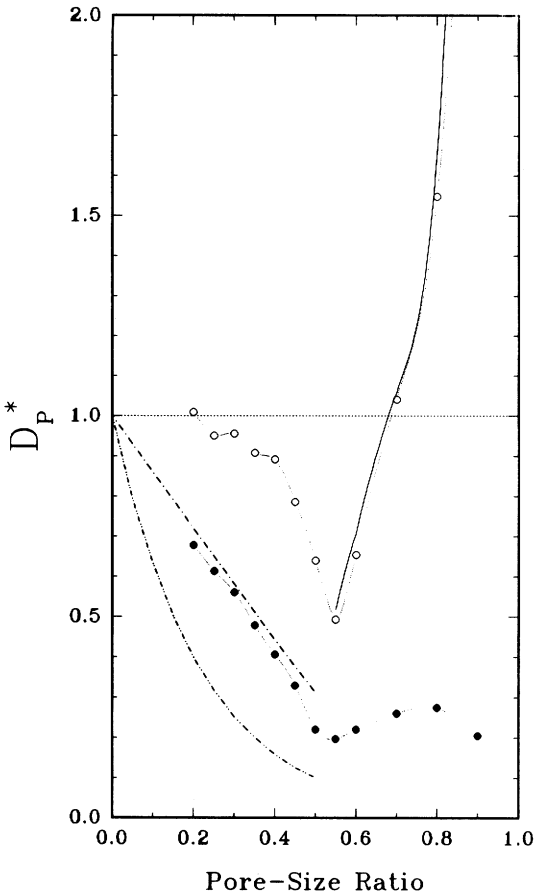

Fig. 1 Reduced axial pore diffusion coefficient as a function of λ: - } - MD results for specular refection; -] - MD results for diffuse reflection; — one-dimensional hard-rod model,
Eq. (3); —-the continuum-mechanical model,
Eq. (4); —-- the empirical equation suggested by Satterfield *et al.*[3]

of hard-sphere fluids confined within a structureless cylindrical hard-wall. As an intermediate between theory and experiment, reliable and unambiguous results obtained from molecular dynamics simulations essentially represent "exact" experimental data. For this reason, this approach will facilitate a direct comparison with experimental and/or theoretical hindered-diffusion results in the literature.

1. Computational Method

The molecular dynamics (MD) method evaluates the trajectories of particles by soplving Newton's equations of motion numerically[6]. For systems of hard-sphere fluids, collision equations can be simplified into algebraic equations since all particles between collisions move in straight lines at constant speed. The MD simulations for pore fluids employed here were similar to those for bulk hard-sphere fluids except in the treatment of particle/pore wall collision at the confining cylindrical hard-wall.

Two scattering conditions to adjust the particle/pore wall momentum are investigated in this work: specular reflection and diffuse reflection. Both conditions conserve the kinetic energy of the colliding particles in the following manner. For specular reflection, the radial velocity components are only changed during a collision by means of elastic scattering. However, the axial component of the particle velocity is the same before and after the wall collision. For diffuse reflection, all the post-collisional velocities are randomly assigned according to the cosine law of diffuse scattering. The resulting diffusion coefficients serve to illustrate the sensitivity of the hindered-diffusion process to the nature of the particle/pore wall interaction.

All simulations were conducted in a fundamental pore cell containing 200 particles. Periodic boundary conditions were imposed at both axial pore boundaries, not only to minimize surface effects but also to approximate an infinite system. Typically, hard-sphere systems are only marginally influenced by the finite system size for a system of 100 particles or more in a fundamental periodic cell[6]. In addition, initial configurations were generated by randomly inserting particles into the cylindrical pore in order to assist in the equilibration of the system. The initial velocities of the particles were randomly chosen from the equilibrium Maxwell-Boltzmann distribution function. Typically, each configuration was aged, or equilibrated, for 100 collisions per particle before accumulating the final ensemble averages of 2000 to 4000 collisions per particle. The intrapore diffusion coefficients were calculated from integration of the velocity autocorrelation functions and from the slope of the mean-square displacement curves versus time.

2. Results and Discussion

The MD simulations were performed at a fixed bulk concentration $n_B^* = 0.5$, where $n_B^* = n_B\sigma^3$ and σ is the hard-sphere diameter. The density condition employed here is close to that corresponding to a liquid phase. For comparison with the corresponding bulk-phase diffusivity, the resulting pore diffusion coefficients are presented in the reduced form

$$D_P^* = \frac{D_P}{D_B} \tag{1}$$

An improved expression, recently reported by Speedy[7], is used to calculate the bulk diffusion coefficients in Eq. (1):

$$D_B = \frac{3\sigma\bar{v}}{8\sqrt{8}\, n_B^*}\left(1 - \frac{n_B^*}{1.09}\right)\left[1 + n_B^{*2}(0.4 - 0.83\, n_B^{*2})\right] \tag{2}$$

where $\bar{v}$ denotes the average particle speed $\sqrt{(8kT/\pi m)}$. This equation is known to be accurate up to a density of $n_B^* = 1.08$.

The simulation results for the axial pore diffusivity are illustrated in **Fig. 1** over a wide range of the pore-size ratio $\lambda = \sigma/d_p$, where d_p is the cylindrical pore diameter. In the case of λ<0.4 for particle/pore wall specular reflection conditions, the pore diffusion coefficients are

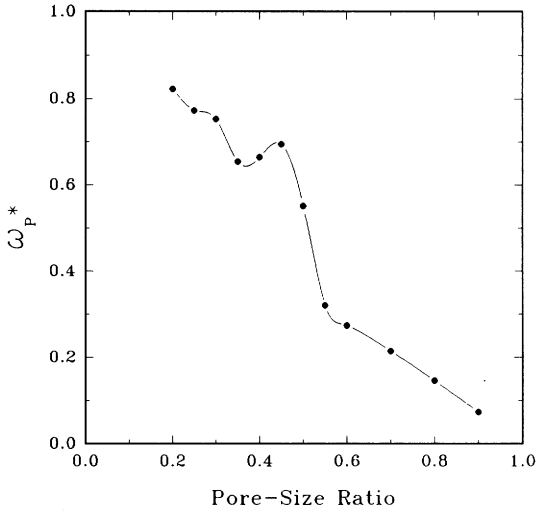

Fig. 2 Reduced particle/particle collision frequency as a function of λ

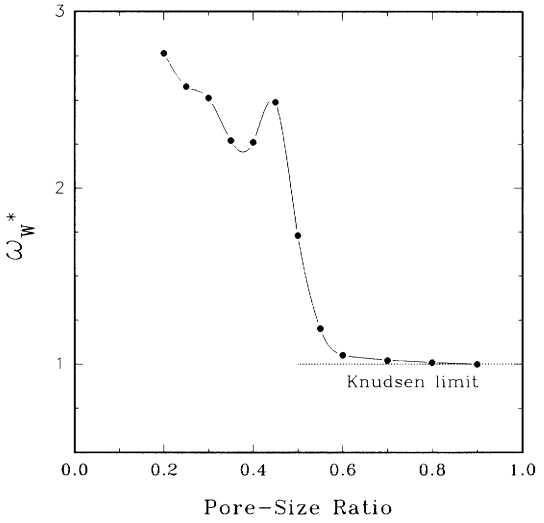

Fig. 3 Reduced particle/pore wall collision frequency as a function of λ

approximately equal to those in an external bulk phase. For $0.2<\lambda<0.4$ the marginal downward trend is primarily due to the increasing influence of hindrance in the pore phase. Between $\lambda = 0.4$ and $\lambda = 0.5$ the pore fluid forms a predominantly monolayer structure extending two particle diameters across the pore. Beyond $\lambda = 0.5$ the actual trajectories of the particles restricted in the cylindrical pores are changed from three-dimensional to pseudo-one-dimensional behavior.

For $\lambda>0.5$ the dynamic properties of pore fluids can be assumed by the character of one-dimensional fluids. The diffusion coefficient in the hard-rod model[8] is exactly given by

$$D_{HR} = \sqrt{(kT/2\pi m)}\left(\frac{1-\rho\delta}{\rho}\right) \tag{3}$$

where ρ and δ are, respectively, the one-dimensional density and finite size of hard-rod fluids. The solid curve shown in this figure represents theoretical approximations predicted by this model. Although the pore diffusion coefficient predicted by Eq. (3) is exact only in the limit $\lambda\rightarrow1$, agreement with the simulation results for specular reflection conditions is seen to be excellent. Under these conditions the microscopic behavior of hard-sphere fluids is much like that of hard-rod dynamics.

In many situations, and particularly in experimental studies of very fine pores[9], a diffusing molecule within pore-matrix solids is observed to be reflected away in random directions except for the case of light molecules (e.g., H_2 or He) in the ideal crystal cleavage planes at low angles of incidence. In this sense, it is reasonable to assume that conditions of diffuse reflection from the pore walls are the more realistic modes of scattering.

The MD results for diffuse reflection exhibit a similar trend to those for specular reflection Short-term memory of the pore fluid is also clearly apparent. However, severe hindrance effects are observed for diffuse reflection, and pore diffusion coefficients are reduced by a factor of two or more compared with specular reflection. In the range $0.4<\lambda<0.5$ the diffusion coefficients decrease sharply since the axial overtaking trajectories are largely restricted by collision sequences. Consequently, the resulting diffusion coefficients pass through a minimum near $\lambda\sim0.5$. For $\lambda>0.5$ the pore diffusivity does not increase as rapidly as that for specular reflection due to backscattering effects in the plane of the pore cross-section. In this case it is expected that the pore diffusion coefficients will asymptotically approach zero in the limit $\lambda\rightarrow1$.

In Fig. 1 we also display the results obtained by an approximation based on the continuum-mechanical model for hindered diffusion of hard-sphere fluids:

$$\frac{D_P}{D_B} = 1 - 1.4033\,\lambda\left[\frac{1+0.5174\,\lambda^5}{1+1.1379\,\lambda^5}\right] \tag{4}$$

This theoretical expression corresponds to the drag correction factor obtained by Haberman and Sayer[4] for a liquid drop of zero viscosity moving in a continuum fluid inside a cylindrical tube. The simulation results are in good agreement with the continuum-mechanical predictions in the range of $\lambda<0.5$. Also shown in this figure are results predicted by a simple empirical equation proposed by Satterfield *et al.*[3], in which the logarithmic values of pore-to-bulk diffusivity were found to be inversely proportional to λ. Even in relatively large pore systems ($\lambda<0.4$) it is observed that this empirical equation predicts a much greater degree of hindrance than the results obtained from the MD simulations.

By expressing the experimental diffusion coefficients in reduced form, one can expect a partial cancellation of the influence of attractive forces in real pore systems. We are of the opinion that this may be the principal cause for the low experimental values of pore diffusion coefficients. Dispersion or polar interactions may have impeded the diffusion process, although no adsorp-

tion excess was observed. This is supported by MD simulation studies for a slit-shaped pore which showed that the diffusion coefficients for a Lennard-Jones Fluid with adsorbing walls[10] are approximately 50% lower than the corresponding diffusion coefficients for a hard-sphere fluid[11]. This is indicative of the influence of attractive interactions on the hindered-diffusion process.

Both particle/particle and particle/pore wall collision frequencies were also determined during the same MD runs. The differences between the two scattering modes of specular and diffuse reflection were found to be negligible. In the case of particle/particle collisions, the simulation results are scaled to the corresponding collision frequencies occurring in the bulk hard-sphere fluids:

$$\omega_P^* = \frac{\omega_P}{\omega_B} \tag{5}$$

The collision frequency per particle in the bulk phase is given by

$$\omega_B = \sqrt{2}\,\pi\,\sigma^2\, n_B\, \bar{v}\, g(\sigma) \tag{6}$$

where the hard-sphere contact radial distribution function $g(\sigma)$ was evaluated using the Carnahan-Starling equation[12].

The particle/pore wall collision frequency is expressed as

$$\omega_W^* = \frac{\omega_W}{\omega_K} \tag{7}$$

In this equation, w_K represents the limiting collision frequency in the Knudsen or free-flow regime, in which the particle trajectories can be determined exclusively by collisions with the pore walls. For a cylindrical pore at this zero density limit $n_B^* \to 0$, one may find that

$$\omega_K = \frac{\bar{v}}{d_P(1-\lambda)} \tag{8}$$

In **Figs. 2** and **3** the MD results of collision frequencies are plotted as a function of λ for particle/particle and particle/pore wall collisions respectively. In the range $0.2<\lambda<0.4$, the particle/particle collision frequencies are substantially lower than the bulk values, while the particle/pore wall collision frequencies are higher than those predicted in the Knudsen limit. In small-pore systems the particle/particle collisions gradually become rare, resulting in a monotonically decaying curve of collision frequencies for $\lambda>0.5$ (Fig. 2). In this case the particle/pore wall collision frequencies rapidly approach the Knudsen limit (Fig. 3).

One of the most interesting features shown in these figures is the peculiar peak observed in the range $0.4<\lambda<0.5$. As we increase λ-values a weakly oscillatory behavior starts to emerge due to the non-continuum structural effects in the cylindrical pores. In this transition region, 'chattering' collisions for particle/particle and particle/pore wall in the plane of the pore cross-section lead to a local maximum. The peak at $\lambda \sim 0.45$ corresponds to incipient close packing of the one-dimensional fluid in the pore. As we decrease bulk concentrations, this peak diminishes and eventually disappears in the ideal gas limit $n_B^* \to 0$. At higher bulk concentrations, however, the local maximum moves upward to the right toward $\lambda \to 0.5$. This result is attributed to the fact that confined hard-sphere fluids in a cylindrical pore tend to structural reordering in the vicinity of the pore wall even though the energetic interactions considered here are only steric exclusions.

Conclusion

In the present work we have reported MD results for system of confined hard-sphere fluids within structureless cylindrical pores. For $\lambda<0.4$ the simulation results of intrapore diffusion coefficients are in good agreement with the continuum-mechanical predictions. Furthermore, in the case of $\lambda>0.5$ it may be assumed that the hard-rod model can provide a reasonable approximation of the diffusive motion of particles. Under these conditions the dynamic properties of hard-sphere fluids in cylindrical pores are related to those for systems of one-dimensional hard-rod fluids. It would be of interest to extent the study to more realistic pore systems in order to verify a number of the conclusions observed in our MD simulations.

Acknowledgment

This research is financially supported by the Korea Science and Engineering Foundation (No. 923-1000-009-1). The authors wish to thank Mr. Woo-Chul Kim for implementing simulation data during this work.

Nomenclature

d_p	=	cylindrical pore diameter	[m]
D	=	diffusion coefficient	[m²/s]
$g(\sigma)$	=	radial distribution function at the contact point	[-]
k	=	Boltzmann constant	
m	=	particle mass	[kg]
n_B	=	number density in the bulk phase	[particles/m³]
$\bar{v}$	=	molecular mean speed	[m/s]
T	=	absolute temperature	[K]
δ	=	hard-rod particle size	[m]
λ	=	pore-size ratio	[-]
ρ	=	density of hard-rod fluid	[particles/m]
σ	=	hard-sphere particle diamerter	[m]
$\omega_P\,\omega_W$	=	particle/particle and particle/pore wall collision frquencies	[collisions/s]

<Subscripts>

B	=	bulk phase
HR	=	hard-rod model
K	=	Knudsen limit
P	=	pore phase

<Superscripts>

*	=	reduced quantity

Literature Cited

1) Nicholson, D. and N. G. Parsonage:"Computer Simulation and the Statistical Mechanics of Adsorption," Academic Press, New York, NY (1982).
2) Dean W. M.: *AIChE J.*, **33**, 1409 (1987).
3) Satterfield, C. N., C. K. Colton and W. H. Pitcher: *AIChE J.*, **19**,

628 (1973).
4) Haberman, W. L. and R. M. Sayer: David Taylor Model Basin Report No. 1143, U. S. Navy Dept., Washington, D. C. (1958).
5) Brenner, H. and L.T. Gaydos: *J. Coll. Interface Sci.*, **58**, 312 (1977).
6) Allen M. P. and D. J. Tildesley: "Computer Simulation of Liquids," Clarendon Press, Oxford (1987).
7) Speedy, R. J.: *Mol. Phys.*, **62**, 509 (1987).
8) Lebowitz, J. L. and J.K. Percus: *Phys. Rev.*, **155**, 122 (1967).
9) Bell, W. K. AND L. F. Brown: *J. Chem. Phys.*, **59**, 3566 (1973).
10) Magda, J., J. M. Tirrell and H. T. Davis: *J. Chem. Phys.*, **83**, 1888 (1985).
11) Antonchenko, V. Ya., V. V. Ilyin, N. N. Makovsky, A. N. Pavlov and V. P. Sokhan: *Mol. Phys.*, **52**, 345 (1984).
12) Carnahan, N. F. and K. E. Starling: *J. Chem. Phys.*, **51**, 635 (1969).